Reprinted from Biochemistry, 1993, 32.

The Asp-His-Fe Triad of Cytochrome *c* Peroxidase Controls the Reduction Potential, Electronic Structure, and Coupling of the Tryptophan Free Radical to the Heme[†,‡]

David B. Goodin* and Duncan E. McRee

Department of Molecular Biology, MB8, The Scripps Research Institute, 10666 North Torrey Pines Road, La Jolla, California 92037

Received September 24, 1992; Revised Manuscript Received December 18, 1992

ABSTRACT: The buried charge of Asp-235 in cytochrome *c* peroxidase (CCP) forms an important hydrogen bond to the histidine ligand of the heme iron. The Asp-His–metal interaction, which is similar to the catalytic triad of serine proteases, is found at the active site of many metalloenzymes and is believed to modulate the character of histidine as a metal ligand. We have examined the influence of this interaction in CCP on the function, redox properties, and iron zero-field splitting in the native ferric state and its effect on the Trp-191 free radical site in the oxidized ES complex. Unlike D235A and D235N, the mutation D235E introduces very little perturbation in the X-ray crystal structure of the enzyme active site, with only minor changes in the geometry of the carboxylate–histidine interaction and no observable change at the Trp-191 free radical site. More significant effects are observed in the position of the helix containing residue Glu-235. However, the small change in hydrogen bond geometry is all that is necessary to (1) increase the reduction potential by 70 mV, (2) alter the anisotropy of the Trp-191 free radical EPR, (3) affect the activity and spin-state equilibrium, and (4) reduce the strength of the iron ligand field as measured by the zero-field splitting. The changes in the redox potential with substitution are correlated with the observed zero-field splitting, suggesting that redox control is exerted through the heme ligand by a combination of electrostatic and ligand field effects. The replacement of Asp-235 with Glu appears to result in a significantly weaker hydrogen bond in which the proton resides essentially with His-175. This hydrogen bond is nevertheless strong enough to prevent the reorientation of Trp-191 and the conversion to one of two low-spin states observed for D235A and D235N. The Asp-His–Fe interaction is therefore as important in defining the redox properties and imidazolate character of His-175 as has been proposed, yet its most important role in peroxidase function may be to correctly orient Trp-191 for efficient coupling of the free radical to the heme and to maintain a high-spin 5-coordinate heme center.

Heme peroxidases form a set of very similar enzymes which catalyze a diverse set of reactions. These enzymes show a common ability to react with H_2O_2 to form an oxidized heme center, which is then used to oxidize the substrate. The diversity arises from the range of substrates that are oxidized by the various enzymes, which include cytochrome *c* (Yonetani, 1976), small-molecule phenols, indoles, and amines (Saunders, 1973), lignin (Tien & Kirk, 1983), manganese (Pribnow et al., 1989; Pease et al., 1989), and even halide ions (Dawson, 1988). To function effectively in oxidative catalysis, the resting states of heme peroxidases are stabilized in the ferric (Fe^{3+}) oxidation state with a 5-coordinate heme center. As a result, these enzymes have unusually negative reduction potentials compared with other heme proteins. It is also likely that, within the class of peroxidases, there is a significant advantage for a particular member to exist with an oxidizing potential that is well matched to its natural substrate. This fine tuning of redox properties would aid in high electron-transfer efficiency and specificity of function. Indeed, the peroxidases are found to exhibit a considerable variability in midpoint potential, from −88 (manganese peroxidase) to −278 mV (horseradish peroxidase) (Millis et al., 1989).

Several features of the surrounding protein structure are believed to contribute to defining the redox properties of heme proteins, including the dielectric environment (Churg & Warshel; 1986, Rees, 1980; Langen et al., 1992) and the electrostatic contribution from nearby charged residues (Rodgers & Sligar, 1991; Varadarajan et al., 1989a,b; Fisher & Sligar, 1985, 1987). For the peroxidases, it is generally believed that the state of the ligand axial to the heme iron is among the most significant mechanisms for control of the redox potential and enzyme reactivity. In cytochrome *c* peroxidase (CCP),[1] the N_ϵ of His-175 serves as the ligand axial to iron and also makes a strong hydrogen bond through N_δ to the buried charge of Asp-235 (Finzel et al., 1984). This constellation of Asp-His-X (see Figure 1) is reminiscent of the catalytic triad in serine proteases (Warshel et al., 1989) and the active site of many zinc enzymes (Christianson et al., 1989; Tainer et al., 1992). A well-positioned carboxylate may significantly influence the properties of the heme active site

† This research was supported by Grant GM41049 from the NIH.

‡ The crystallographic coordinates for the structures presented in this work have been deposited with the Protein Data Bank, Chemistry Department, Brookhaven National Laboratory, Upton, NY 11973, from which copies are available (entries P1CCA, P1CCB, and P1CCC).

* Author to whom correspondence should be addressed.

[1] Abbreviations: CCP, cytochrome *c* peroxidase; CCP-CN, cytochrome *c* peroxidase cyanide complex; CCP(MKT), cytochrome *c* peroxidase produced by recombinant expression in *E. coli* containing Met-Lys-Thr at the N-terminus; cyt c, cytochrome *c*; D235A, mutant in which Asp-235 is replaced by Ala; D235E, mutant in which Asp-235 is replaced by Glu; D235N, mutant in which Asp-235 is replaced by Asn; EPR, electron paramagnetic resonance; ES, the H_2O_2 oxidized state of CCP; HRP, horseradish peroxidase; MES, 2-(*N*-morpholino)ethanesulfonic acid; MOPS, 3-(*N*-morpholino)propanesulfonic acid; MPD, 2-methyl-2,4-pentanediol; NBS, National Bureau of Standards; PO, peroxidase; Tris, tris(hydroxymethyl)aminomethane.

0006-2960/93/0432-3313$04.00/0

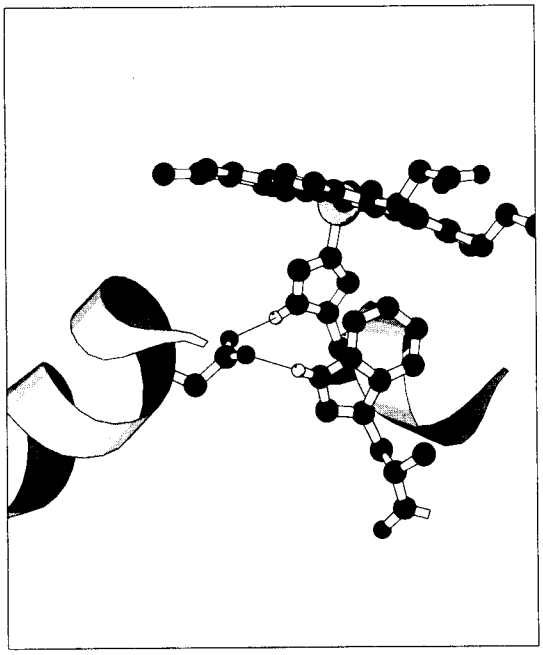

FIGURE 1: View of the Asp-His-Fe triad of cytochrome *c* peroxidase. Hydrogen bonds are indicated between Asp-235 and both the His-175 ligand and the Trp-191 free radical center. The molecular model was obtained from the refined coordinates of the *E. coli* derived enzyme CCP(MKT), and the figure was generated using MOLSCRIPT (Kraulis, 1991).

either by electrostatic stabilization of the positive charge on iron or by partial (or complete) deprotonation of the histidine to form the imidazolate, thereby increasing the strength of the histidine–iron bond. In contrast to the peroxidases, most other heme proteins with an axial histidine ligand have a relatively weak hydrogen bond between the histidine and a peptide backbone carbonyl (Valentine et al., 1979).

Many results have combined to provide a consistent picture in which the Asp-His interaction of CCP serves to deprotonate the histidine significantly to provide a strong axial ligand with imidazole character. Early proposals of this effect (Finzel et al., 1984; Valentine et al., 1979) have been borne out by studies of model heme complexes, which have demonstrated the importance of the axial ligand hydrogen bond to ligand binding kinetics (Swartz et al., 1979), metal–ligand bond strength (Stein et al., 1980), reduction potential (Doeff et al., 1983), and reactivity (Traylor et al., 1984; Groves & Nemo, 1983; Lee et al., 1985). Studies on CCP itself, in which the Asp-His interaction is severed by the D235N mutation, have resulted in the observation of an altered resonance Raman mode in the Fe^{2+} enzyme associated with the His–Fe bond (Smulevich et al., 1988; Spiro et al., 1990). In the low-spin Fe^{3+}–CN complex, this mutation was observed to alter paramagnetically shifted resonances assigned to His-175, indicating that effects of the hydrogen bond are propagated onto the His-175 ligand (Satterlee et al., 1990). These studies have provided important insights into the properties of this interaction, but due to experimental necessity, they have been carried out on nonnative states (Fe^{2+} and CN complex) of the enzyme. In addition, it has been shown (Wang et al., 1990) that the D235N mutation introduces a significant rearrangement of the free radical center, Trp-191 (Sivaraja et al., 1989), which lies in contact with His-175. This could introduce complications in the interpretation of the role of this sensitive hydrogen bond in the native state. Thus, the effect of this hydrogen bond on the redox properties or electronic structure of any heme enzyme in its native Fe^{3+} state remains unexamined. It is also unclear to what degree the redox potential may be tunable by modulation of this interaction. We report studies on three mutant of Asp-235 in CCP and show that manipulation of this interaction has a direct effect on the iron zero-field splitting, significantly alters the electrochemical properties of the enzyme, and changes the nature of the coupling of the Trp-191 free radical with the heme center.

MATERIALS AND METHODS

Protein Expression and Purification. Mutants of CCP were constructed in the *Escherichia coli* expression plasmid pLACCCP2-8 by oligonucleotide site-directed mutagenesis of single-stranded DNA containing uracil, and the full coding region for each mutant was verified by DNA sequencing (Goodin et al., 1991). apo-CCP was overexpressed and purified from 4–L cultures of *E. coli* HB2151 before heme reconstitution to give the holoenzyme as described earlier (Goodin et al., 1991). Purified enzyme was recrystallized twice from distilled water and stored as a crystal suspension at 77 K. For use, crystals were washed in cold distilled water and dissolved in the appropriate buffer. Protein concentrations were determined from the molar absorptivities ($\epsilon_{408}^{CCP(MKT)}$ = 101 mM^{-1} cm^{-1}; $\epsilon_{411}^{D235A} = \epsilon_{411}^{D235N}$ = 97 mM^{-1} cm^{-1}; ϵ_{411}^{D235E} = 100 mM^{-1} cm^{-1}) as determined from the pyridine hemochromogens (Nicola et al., 1975). Wild-type CCP or CCP(MKT) refers to the protein produced from the cloned gene sequence and contains Ile-53, Gly-152, and Met-Lys-Thr at the N-terminus (Goodin et al., 1991).

Steady-State Kinetics. Kinetics for the CCP-catalyzed oxidation of reduced horse heart cytochrome *c* by H_2O_2 was carried out at 25 °C in 20 mM Tris/phosphate (pH 6.0), 25 μM reduced cyt c, 100 μM H_2O_2, and 250–2500 pM CCP as described earlier (Goodin et al., 1987, 1991).

Optical and EPR Spectroscopy. UV/visible spectra were collected at 25 °C using a Hewlett-Packard 8452A diode array spectrophotometer in the stated buffer. EPR spectra were collected in either 100 mM MES (pH 5) or 100 mM MOPS (pH 7) and contained 60% glycerol unless otherwise stated. Spectra were collected on a Bruker ESP300 spectrometer equipped with an Air Products LTR3 liquid helium cryostat at 9.51 GHz. Instrument settings are given in the figure legends.

X-ray Crystallographic Analysis. Single crystals of CCP(MKT), D235E, and D235A were grown from 30% 2-methyl-2,4-pentanediol (Wang et al., 1990). Data for CCP(MKT) and D235A were collected at 15 °C on a Siemens three-axis goniometer/area detector. For D235E, a Siemens four-circle area detector was used. In each case, a single crystal was used to collect the entire data set to minimize scaling errors, and the data collection time was completed within 48 h. The reflection intensities were integrated using XENGEN (Howard et al., 1987) and gave data sets that contained 23 924 unique reflections (85% complete to 1.7 Å, R_{sym} = 4.75%) for CCP(MKT), 16 525 unique reflections (76% complete to 2.1 Å, R_{sym} = 10.1%) for D235E, and 20 656 unique reflections (83% complete to 2.0 Å, R_{sym} = 5.6%) for D235A. The unit cell parameters determined for CCP(MKT) (space group $P2_12_12_1$, a = 105.2 Å, b = 74.3 Å, c = 45.4 Å) were similar to those reported earlier for CCP produced in *E. coli* (Wang et al., 1990). Initial solution of the CCP(MKT) structure was obtained by molecular replacement using the program XPLOR (Brünger et al., 1987). A rotation/translation probe was constructed from the yeast CCP model (Finzel et al., 1984) by replacing Thr-53 with Ile and Asp-152 with Gly. The model resulting from the rotation/translation search was

refined to 1.8-Å resolution and an R value of 21% for all data between 5.0 and 1.8 Å (R = 19% for all data between 5.0 and 2.1 Å). During this process, surface side chains, which were omitted from the yeast CCP structure due to disorder (Finzel et al., 1984), were included as their density was clearly visible in the map. The final refined model for CCP(MKT) included 49 water molecules and was refined using isotropic B values. Data for D235E and D235A were merged and scaled with the wild-type structure factors to construct Fourier difference maps. The initial models for D235E and D235A were constructed from these difference maps using the program XFIT (McRee, 1992) and were refined by at least two cycles, each consisting of geometry-restrained least-squares refinement with XPLOR (Brünger et al., 1987) followed by manual adjustment. Final refinement for the mutant models gave R values of 19% for data between 5.0 and 2.1 Å for D235E and 19% for all data between 5.0 and 2.0 Å for D235A.

Potentiometric Titrations. Anaerobic reductive titrations were performed using a method adapted from those previously reported (Stankovich, 1980; Conroy et al., 1978). A 3-mL solution of approximately 5 μM CCP in buffer containing 1 mM methyl viologen and 1 μM phenosafranin as redox mediator was sealed in an air-tight cuvette and continuously flushed with a stream of scrubbed N_2. The cell was equipped with an Au foil working electrode, a Pt wire counter electrode, and a Ag|AgCl reference electrode. The latter two electrodes were isolated from the solution by a double salt bridge, and the potential of the Ag|AgCl electrode was calibrated against a standard calomel electrode. The spectrophotometer (Hewlett-Packard 8452A), potentiostat (Princeton Applied Research Model 363), and temperature monitor were interfaced to a personal computer which controlled the automated redox titrations. It is important to maintain anaerobic conditions in the cell to prevent O_2 binding by the reduced enzyme. Thus, all buffers were degassed and flushed with scrubbed N_2 before use. An advantage of the titration method employed is that reduced methyl viologen, which is the electron-transfer mediator, can be used to complete the removal of O_2 from the cell. All components except the enzyme were first sealed in the cell, and small quantities of reduced methyl viologen were produced electrochemically at the working electrode. After equilibration, the procedure was repeated as necessary until small amounts (~300 nM) of reduced methyl viologen could be maintained for >0.5 h. The CCP sample was then introduced through an injection port for the titration. For each point, a small quantity (approximately 250 pmol) of methyl viologen was reduced at the working electrode by transiently applying 8 μA across the working and counter electrodes, followed by an equilibration period. After the potential had stabilized (approximately 10–15 min), the optical spectrum and the potential between the Au and reference electrodes were recorded. Midpoint potentials were determined from the Nernst equation by least-squares fitting of the absorbance at 438 nm versus the measured potential corrected to the standard hydrogen electrode (SHE). The Nernst slopes for all data on CCP(MKT) reported in this study had a mean of 58.4 mV.

Measurement of the Fe^{3+} Zero-Field Splitting. A high-spin ferric heme in a weak axial ligand field will have an $S = {}^5/_2$ ground spin state. This state will be split in the absence of a magnetic field by the crystal field potential into three sets of Kramers doublets ($m_s = \pm{}^1/_2, \pm{}^3/_2, \pm{}^5/_2$) that are separated in energy by $2D$ and $4D$, respectively. Several methods have been used to measure the zero-field splitting parameter (D), including Mössbauer (Schulz et al., 1984), magnetic circular dichroism (Stephens, 1976), and EPR (Scholes et al., 1971; Colvin et al., 1983). We have used the latter technique of measuring the temperature dependence of the electronic spin-lattice relaxation by EPR. Of the processes that contribute to the relaxation between the $m_s = \pm{}^1/_2$ states observed by EPR of high-spin hemes, it is known that the phonon-mediated thermal excitation to the $m_s = \pm{}^3/_2$ manifold, or Orbach process, dominates (Schulz et al., 1984; Colvin et al., 1983).

Relative magnitudes of $1/T_1$ were obtained by progressive saturation of the ferric EPR signals (Hoffman et al., 1981). Samples were approximately 400 μM protein in 100 mM MES/MOPS (pH 5 or 7) and 60% glycerol. For these measurements, EPR signals were measured using a 1.56-kHz field modulation of 5 G. Temperatures below 4 K were obtained by maintaining reduced pressure in the sample cryostat and determined from a calibration curve of pressure vs temperature. This curve was constructed from control sample tubes containing an NBS-certified Ga–As diode calibrated to ±0.05 deg from 2 to 4 K. The rhombic signal measurements were made at g_x = 6.59 (1033.2 G) and the axial signal measurements (reported in the text) were made at $g_\perp$ = 6.1 (1110.6 G). At a given temperature (T), the signal amplitude (S) as a function of microwave power (P) was fit to $S/P^{1/2} = K/(1 + P/P_{1/2})^{1/2}$ to give the constant, K, and the half-saturation power, $P_{1/2}$. Values of $P_{1/2}$ versus sample temperature were fit to $P_{1/2} \propto (1/T_1) = AT + BT^9 + C(2D/k)^3 e^{(-2D/kT)}$, where the three terms represent the direct, Raman, and Orbach relaxation processes, respectively, and A, B, and C are constants (Abragam & Bleaney, 1986). By fitting the data to each of the terms individually, we observed that only those which included the Orbach process were satisfactory, indicating that the Orbach mechanism dominates the relaxation between 2 and 4 K. This is consistent with studies of Schulz et al. (1984), who have shown for horseradish peroxidase that the contribution from Raman relaxation is insignificant below 160 K. Thus, to determine $2D/k$, only the Orbach term was retained, and all data were fit to $\ln(P_{1/2}) = \ln(C) + 3\ln(2D/k) - (2D/k)(1/T)$, where C was fixed at 0.12 as determined for wild-type CCP.

RESULTS

Coordination, Spin State, and Activity. The coordination and functional properties of the mutants D235N and D235A are significantly altered, while D235E is unique in retaining many of the characteristics of wild-type CCP. Initial turnover rates for the CCP-catalyzed oxidation of horse heart cytochrome c (Sigma Type VI) were 293, 0, 0, and 120 (± 0.3) s^{-1} for wild-type CCP, D235N, D235A, and D235E, respectively. Thus, while D235N and D235A are unable to effectively catalyze cytochrome c oxidation (<0.1% of wild-type CCP activity), D235E retains 41% of the activity of wild-type enzyme. A similar pattern is observed in the ease with which these mutants undergo the high- to low-spin-state transition. Shown in Table I are the absorbance features characteristic of this transition. The charge-transfer (CT) transitions at 506 and 646 nm observed for the 5-coordinate high-spin state of CCP(MKT) are invariant between pH 5 and 7 in acetate and phosphate buffers. Both D235N and D235A are converted with increasing pH from a 6-coordinate high-spin (hs) form, characterized by CT bands at 496 and 622 nm, to a low-spin species (ls1) with pK = 5.2 (titration not shown), consistent with results reported for a D235N mutant (Smulevich et al., 1991; Vitello et al., 1992). This ls1 species, in which the CT1 transition is not evident and β/α bands are observed at 538 and 575 nm, respectively, has been

Table I: Visible Absorption Maxima (nm) Characteristic of the pH-Dependent Spin-State Conversion of Asp-235 Mutants

CCP variant	condition	CT1	CT2	β	α
CCP(MKT)	KOAc, pH 5	506	646		
D235E		504	628		
D235N		496	622	540	575 (sh)
D235A		496	622	538	575 (sh)
CCP(MKT)	KP_i, pH 6	508	645		
D235E		504	630	534 (sh)	
D235N			622	538	575
D235A			622	536	575
CCP(MKT)	KP_i, pH 7	510	645		
D235E				534	562
D235N				532	562
D235A				531	563

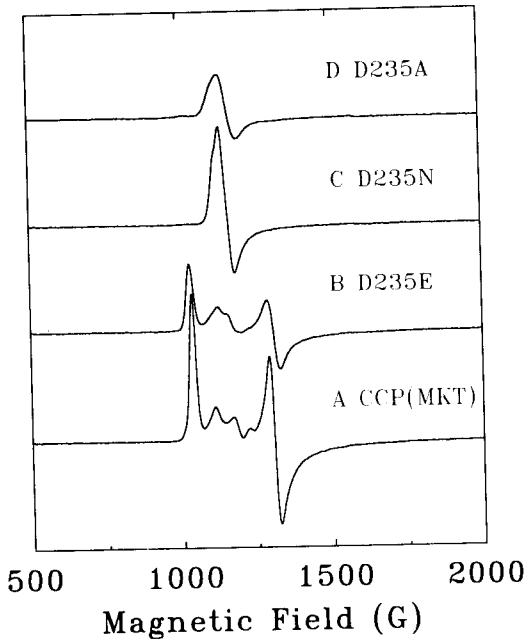

FIGURE 2: EPR spectra of the native ferric state of CCP(MKT) and Asp-235 mutants. Shown are samples of CCP(MKT) (A), D235E (B), D235N (C), and D235A (D). Spectra were collected at 10 K using a Bruker ESP 300 spectrometer operating at X-band (9.52 GHz), 2-mW microwave power and 100-kHz field modulation of 5-G amplitude. Proteins were approximately 300 μM in 100 mM MOPS (pH 7) and 60% glycerol.

suggested to result from the deprotonation of the bound axial water to give the hydroxyl–ferriheme complex (Smulevich et al., 1991; Vitello et al., 1992). A further increase in pH results in the conversion (pK = 6.8) of D235N and D235A to a second low-spin species (ls2), characterized by β and α bands at 532 and 562 nm, respectively. The distinction between these two low-spin forms has been noted previously for a D235N mutant, and it was suggested that this conversion is associated with the replacement of the hydroxyl ligand with the distal His-52 as the sixth heme ligand (Smulevich et al., 1991; Vitello et al., 1992). However, we observe that D235E is predominantly in the 6-coordinate high-spin state at pH 5, where D235N and D235A are roughly equal mixtures of the hs and ls1 forms. Upon raising the pH, D235E appears to convert directly to the ls2 form at pH 7 without exhibiting the features associated with the intermediate low-spin rate, ls1 (see Table I). Finally, Figure 2 shows low-temperature EPR spectra in the g = 6 region for the ferric state of CCP(MKT) and the Asp-235 mutants at pH 7 in 60% glycerol. These spectra show that under these conditions D235E exhibits the rhombically distorted axial high-spin EPR signal characteristic of the wild-type enzyme, wild D235N and D235A show only the axial g = 6 species. This native-like signal of D235E requires the presence of glycerol, as in its absence each of the mutants displays the axial species.

Structural Effects of Asp-235 Mutants. The spectroscopic and functional properties suggest that the hydrogen bond to N_δ of His-175 may remain intact in the D235E mutant, and they also suggest more pronounced structural alterations for D235N and D235A. In addition, the possibility of unanticipated structural alterations must be carefully considered. Indeed, an unexpected reorientation of Trp-191 has been observed for a D235N mutant (Wang et al., 1990) of CCP. For this reason, it is important to characterize the structural effects of the mutants reported here in detail. This was accomplished by the determination of the X-ray crystal structures of CCP(MKT), D235E, and D235A. The 1.8-Å structure obtained for CCP(MKT) by molecular replacement and refinement included surface side chains missing in the yeast CCP structure (Finzel et al., 1984), as their presence was indicated in the electron density maps. The refined structure was otherwise essentially identical with that reported previously for the *E. coli* derived enzyme (Wang et al., 1990).

The difference Fourier map (Figure 3) of D235E indicated very little alteration in the structure near the active site, but showed significant movement of the helix backbone bearing Glu-235. Examination of the refined models of CCP(MKT) and D235E (Figure 4) shows that in spite of the additional CH_2 group of the glutamate side chain, the substitution introduces only small changes in the position of the carboxylate of residue 235 and its hydrogen-bonding partners, His-175 and Trp-191. There is correspondingly little change in the structure of the heme or the residues in the distal binding pocket. The $O_{\delta 1}$ oxygen of Glu-235 moves 1.1 Å in a direction toward His-175 and away from the heme, resulting in a small but significant rotation of His-175 about the histidine–iron bond. This rotation maintains the 3.0-Å distance observed for the Asp-235 to His-175 hydrogen bond, but the geometry of the interaction is slightly altered, as seen in Figure 4. No significant difference is evident in the Fourier difference map near Trp-191 (Figure 3b) or in its refined position (Figure 4). These small changes at the active site are in contrast to a significant movement of Met-172 and a shift in the position of the entire helix bearing residue 235. The additional side-chain carbon of Glu-235 is accommodated by a significant rearrangement in its side-chain conformation. This results in a reduced occupancy of the ordered water, which forms hydrogen bonds to Asp-235, and a reorientation of the Met-172 side chain in which C_δ moves by 1.7 Å. The C_α main chain of D235E is pushed back 1.2 Å by the more extended side chain of the substituted Glu, resulting in a coordinated movement of helix H from Pro-233 to Pro-242 with an average C_α displacement of 0.7 Å. This movement may be interpreted as a small shift and rotation of the helix viewed as a rigid body with the two prolines as hinge points. It is noteworthy that each of these large changes in the Glu-235 side chain and helix is accompanied by significantly higher refined B values compared to the wild-type structure. For example, the average B values for the atoms in Asp-235 and Glu-235 are 11.3 and 29.6, respectively.

In contrst to D235E, the D235A mutation results in an entirely different structural effect on the enzyme. As shown in Figure 5, the most significant effect of the D235A mutation is in the reorientation of Trp-191, which has flipped over to create a new 2.75-Å hydrogen bond between the Trp-191 indole NH and the backbone carbonyl of Leu-177. The nature of this reorientation is entirely analogous to that observed for a

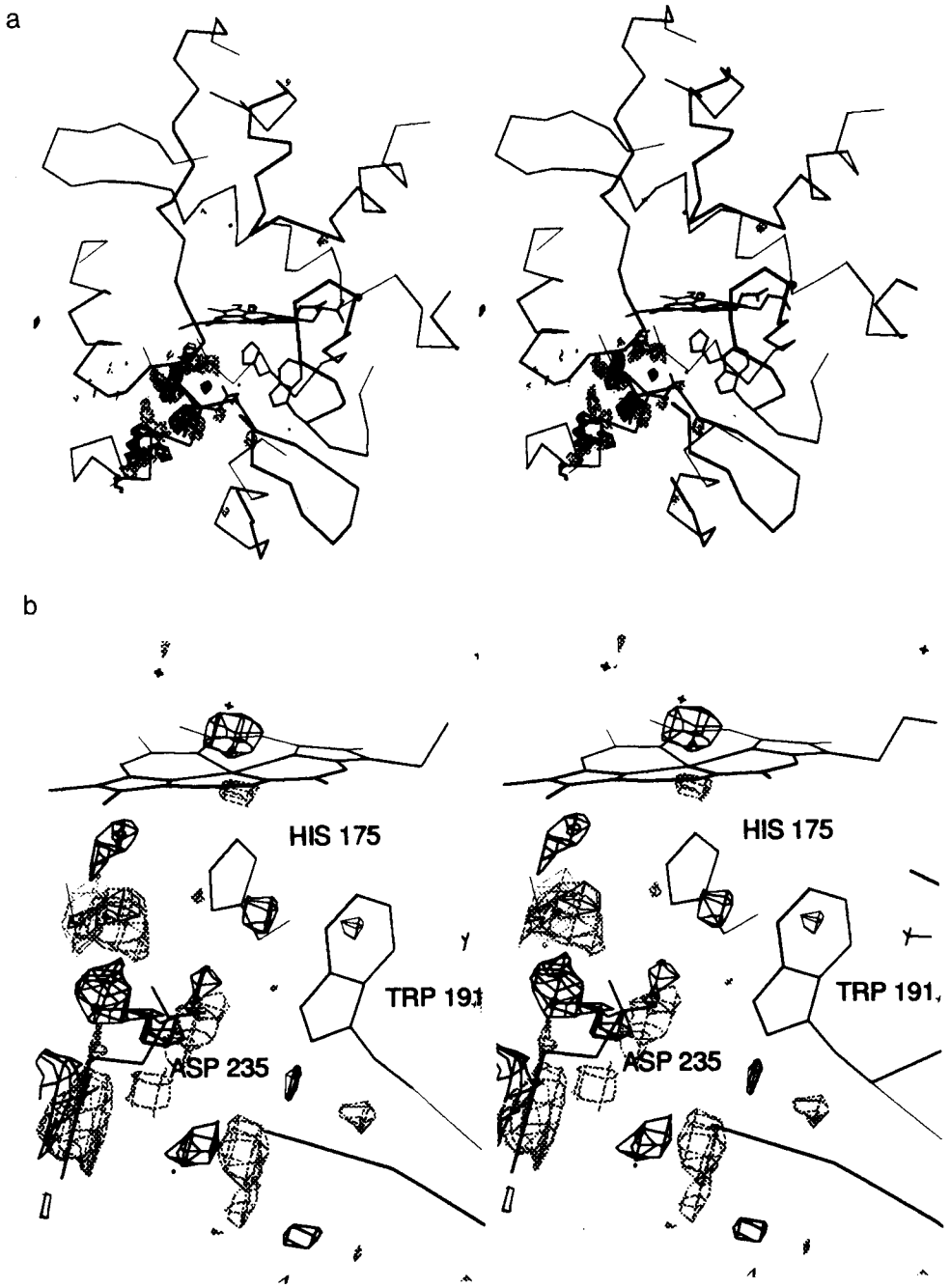

FIGURE 3: Stereoviews of the Fourier difference map at 2.1 Å for D235E minus CCP(MKT). The model coordinates are those of the 1.8-Å structure of CCP(MKT). Positive difference density is shown in black and negative density in gray. An overview of the map is shown contoured at $\pm 4\sigma$, which illustrates the observed changes of the helix bearing the Glu-235 (a). A close-up view of the active site contoured at $\pm 3\sigma$, which shows little perturbation of the proximal His-175 or Trp-191 (b). There is some evidence on the distal heme face for a small movement of the iron into the heme plane and/or coordination by the distal H_2O.

D235N mutation (Wang et al., 1990). These authors also noted small alterations in the distal cavity of D235N, including the movement of the distal H_2O to a position suggesting direct ligation to the iron in D235N. Although we observe significant ($>3\sigma$) positive difference electron density above the iron in both D235E and D235A (see Figure 3b), indicating some movement of the iron into the heme plane or coordination by the distal H_2O, the resolution of the mutant structures (2.1 Å) is insufficient to make definite conclusions about changes in the distal H_2O positions. It is clear, however, that the proximal differences observed for D235N or D235A on one hand and D235E on the other demonstrate the importance of the charged hydrogen bond in maintaining the geometry of these active site residues.

The Trp-191 Free Radical. In spite of the very subtle perturbation of the structure near the active site and the intermediate effects on the coordination state and activity of the D235E mutant, we observe evidence that the nature of the coupling between the Trp-191 free radical and the heme has been significantly altered. EPR spectra collected at 10 K for the ES complexes are shown in Figure 6. It is clear that the Trp-191 free radical species of wild-type CCP, which shows axial symmetry with an apparent $g_\parallel > g_\perp$, has been altered by the mutation to give a signal which also displays axial anisotropy but with the opposite sense (i.e, with $g_\parallel < g_\perp$). The power saturation properties of the free radical derived from D235E at various temperatures between 4 and 50 K (data not shown) show that this radical does not arise from the narrow,

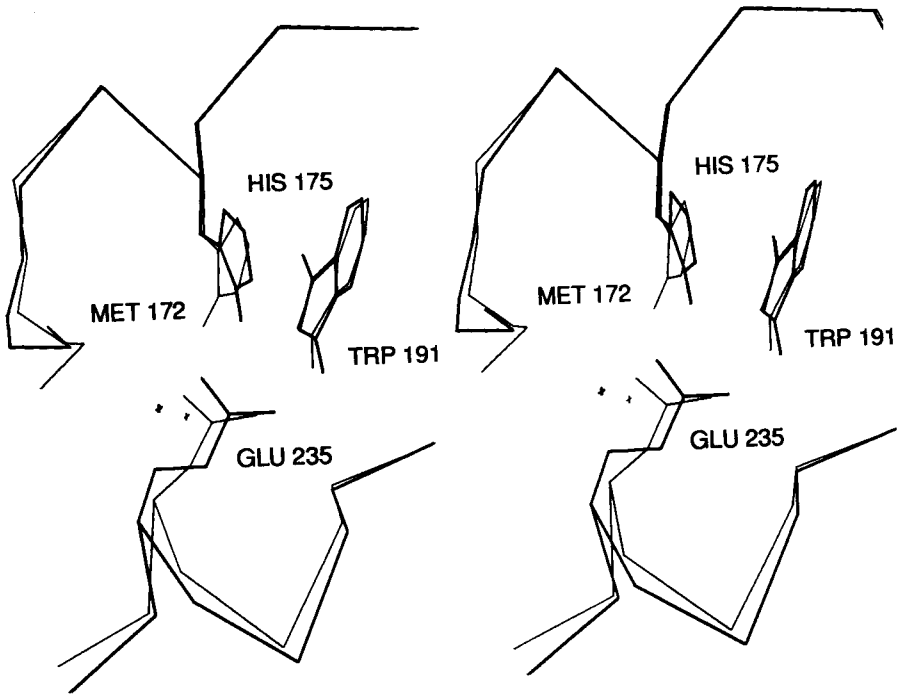

FIGURE 4: Stereoview of the active site residues in the refined crystal structures of wild-type CCP(MKT) (thin lines) at 1.8-Å resolution and the D235E mutant (thick lines) at 2.1-Å resolution. The view is from the direction of the heme, looking down onto the proximal His-175 ligand. The position of the water molecule which is found with reduced occupancy in D235E is indicated by the cross mark. The substitution causes a small movement of the Glu-235 carboxylate and rotation of His-175. Although the His(N_δ)–Glu($O_{\delta 1}$) distance remains 3.0 Å, the geometry of the hydrogen bond is distorted. The side-chain conformation of Met-172 is altered, but the mutation has little effect on Trp-191 or the other residues in the active site.

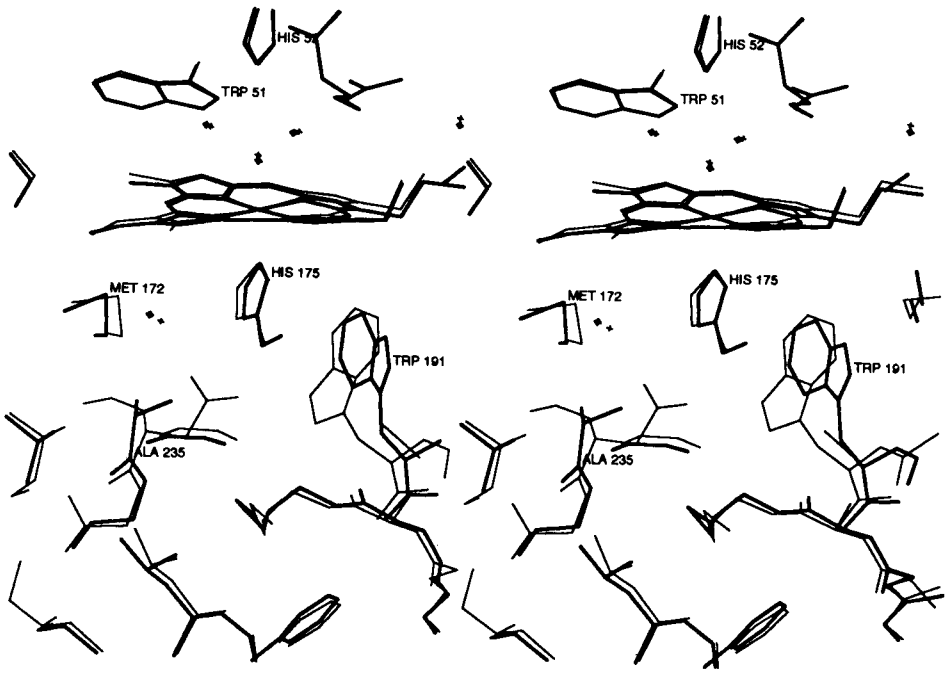

FIGURE 5: Stereoview of the refined crystal structure at 2.0 Å of D235A (thick lines) overlaid on the structure of CCP(MKT) (thin lines). The most significant change is a reorientation of the Trp-191 ring in a manner analogous to that observed for the D235N mutation (Wang et al., 1990).

isotropic minority signal that is easily saturable and known to be a species other than Trp-191 (Goodin et al., 1987). In addition, no hyperfine structure could be resolved by CW EPR on this signal at low power and modulation amplitude, which also indicates that the signal is not associated with the minority signal (Hori & Yonetani, 1985; Goodin et al., 1987; Fishel et al., 1991). Instead, this signal is similar to the Trp-191 radical of wild-type CCP in that it is difficult to saturate even at 10 K and thus is presumably coupled to the $S = 1$ oxyferryl heme iron center. Finally, ENDOR spectra (Houseman et al., 1993) of this species clearly indicate that the radical observed with D235E contains the proton hyperfine pattern characteristic of the Trp-191 radical of wild-type enzyme. Upon addition of a stoichiometric quantity of H_2O_2 to D235N and D235A, we observe incomplete reaction and formation of a small, substoichiometric quantity of a narrow EPR signal at $g = 2$ that is similar to that reported earlier for D235N (Fishel et al., 1991).

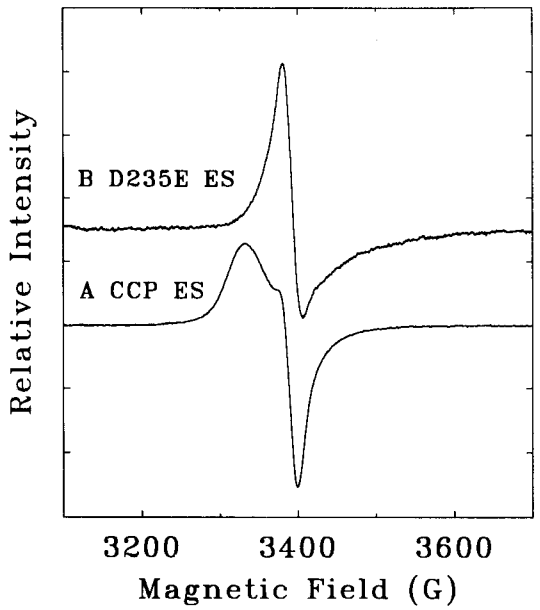

FIGURE 6: EPR spectra at 10 K for the Trp-191 free radical species of compound ES. Spectra are shown for CCP(MKT) (A) and D235E (B). Samples were 0.4 mM enzyme in 100 mM KP_i (pH 6.0) to which H_2O_2 was added to a 1 mM final concentration. Instrumental conditions were 2-mW power at 9.51 GHz, with 100-kHz field modulation of 5-G amplitude.

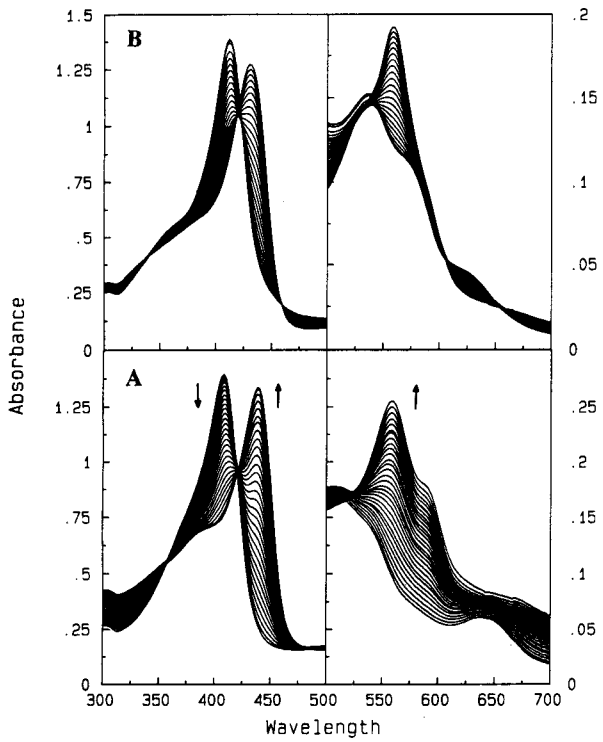

FIGURE 7: Potentiometric titration of CCP(MKT) and D235N cytochrome *c* peroxidase. Reductive titrations were performed at 15 °C in 100 mM potassium phosphate (pH 7.0). Optical spectra collected during the course of the reduction are shown for wild-type CCP (A) and D235N (B). The directions of the arrows represent formation of the ferrous enzyme. Midpoint potentials were determined from the Nernst equation by least-squares fitting of the absorbance at 438 nm versus the measured potential corrected to the standard hydrogen electrode (SHE). The midpoint potentials were −182.3 and −78.5 mV for CCP(MKT) and D235N, respectively.

Reduction Potentials. Reductive titrations at pH 7 are shown for CCP(MKT) and D235N in Figure 7. The titration for D235N shows the conversion from the ls2 form of the Fe^{3+} enzyme to the 5-coordinate Fe^{2+} state with λ_{max} values at 435 and 558 nm. By comparing the spectra at the end of titrations

Table II: Zero-Field Splitting Parameters and Reduction Potentials of CCP Mutants

enzyme	$2D/k$ (K)	E_m^7 (mV)
rhombic component		
HRP	32.5	−278[a]
CCP(MKT)	29.6	−183
D235E	26.7	−113
axial component		
CCP(MKT)	23.2	
D235E	23.4	
D235N	21.6	−79
D235A	22.3	−78

[a] Makino et al., 1976.

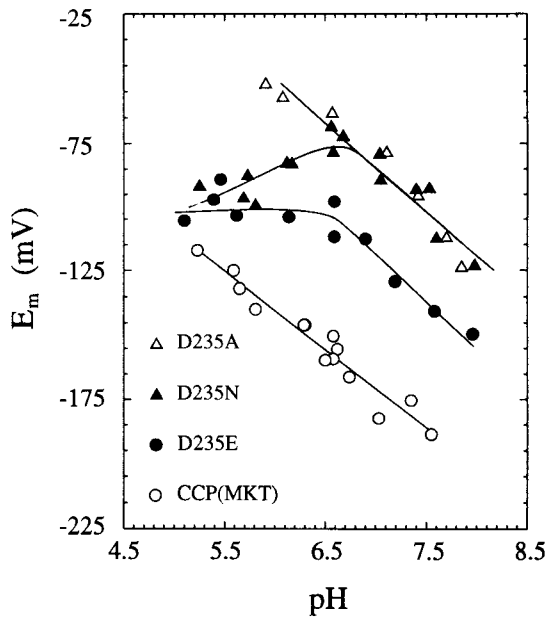

FIGURE 8: Midpoint reduction potential as a function of pH for CCP(MKT) (○), D235N (▲), D235A (△), and D235E (●). Potentials were determined as described in Figure 7, and pH values were measured after the titration. The pH range of the data was limited at high pH by protein stability and at low pH by long equilibration times.

performed over a range of pH values, the Fe^{2+} state of D235N was observed to undergo a transition with pK = 7.6 to a form with λ_{max} = 526, 530, and 560 nm. This corresponds to the two-proton ionization associated with the 5-coordinate to 6-coordinate transition observed in the reduced states of both wild-type CCP and D235N (Miller et al., 1990; Conroy et al., 1978).

Disruption of the Asp-235 hydrogen bond to His-175 has a dramatic effect on the redox potential of CCP. As shown in Table II, we observe that the midpoint reduction potential (Fe^{2+}/Fe^{3+}) at pH 7 shifts from −182 mV for the wild-type enzyme to −79, −78, and −113 mV for D235N, D235A, and D235E, respectively. Thus, as before, we see the most dramatic effect upon completely disrupting the carboxylate–histidine interaction (D235N and D235A) and an intermediate effect for the D235E mutant. The redox potential of heme peroxidases decreases with increasing pH, indicating that reduction of Fe^{3+} is accompanied by the protonation of an unknown group (Millis et al., 1989; Conroy et al., 1978; Ricard et al., 1972; Harbury, 1957). This characteristic is observed for each the mutants above pH 6.5 as shown in Figure 8. However, an ionization of the oxidized state with a pK of 6.5 is observed for the D235E and D235N mutants, and the potentials become relatively independent of pH below this value. Some indication of similar behavior is present in the

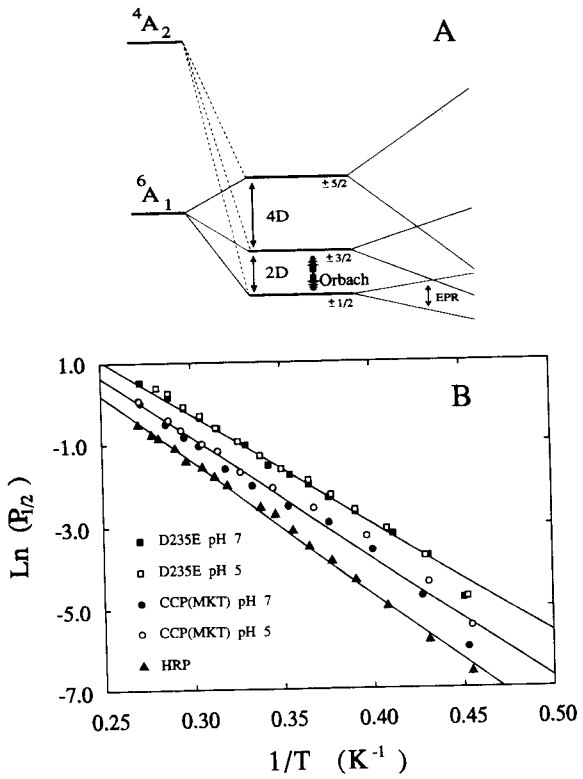

FIGURE 9: Effects of Asp-235 mutation on the Fe^{3+} zero-field splitting measured for the rhombic EPR signal (A). A strong histidine bond could significantly increase the axial ligand field, which would decrease the energy to the lowest excited quartet state ($^4A_2$). Increased mixing with the ground state would result in larger values of the zero-field splitting parameter ($2D$). Above 2 K, electronic spin-lattice relaxation ($1/T_1$) in high-spin ferric heme proteins is dominated by the Orbach mechanism, which proceeds via phonon-induced excitation of low-lying excited spin states (Schulz et al., 1984; Colvin et al., 1983). Measurement of $2D$ for HRP (lower), wild-type CCP (middle), and D235E (upper) from the temperature dependence of Orbach spin-lattice relaxation (B). Relative magnitudes of $1/T_1$ were obtained by progressive saturation of the ferric EPR signals (Hoffman et al., 1981). Samples were approximately 400 μM protein in 100 mM MES/MOPS (pH 5, open symbols, or pH 7, filled symbols and 60% glycerol. The data for a given sample were essentially identical at the two pH values. Thus, for analysis, the two data sets at different pH values were combined. The rhombic signal measurments were made at $g_x = 6.59$ (1033.2 G). At a given temperature (T), the signal amplitude (S) as a function of microwave power (P) was fit to $S/P^{1/2} = K/(1 + P/P_{1/2})^{1/2}$ to give the constant, K, and the half-saturation power, $P_{1/2}$. To determine $2D/k$, these data were fit to $\ln(P_{1/2}) = \ln(C) + 3\ln(2D/k) - (2D/k)(1/T)$, where C was fixed at 0.12 as determined for wild-type CCP (see Materials and Methods). Values thus obtained for $2D/k$ are shown in Table II.

E_m vs pH curve of D235A, although the break is not as clearly defined.

Fe^{3+} Zero-Field Splitting. Measurements of the zero-field splitting parameter (described in Materials and Methods) were made for wild-type CCP and Asp-235 mutants in their high-spin ferric states. Relative values of the spin-lattice relaxation rate ($1/T_1$) obtained from saturation data are shown in Figure 9 as a function of temperature for wild-type CCP and for D235E. These data were measured at the $g_x = 6.6$ component of the high-spin rhombic signal observed for these species in the presence of glycerol. The data of Figure 9 show that no differences were observed for samples prepared at pH 5 and 7. This is to be expected, because even though the relative ratios of the rhombic and axial high-spin signals varied with pH, the rhombic signal at both pH values should represent the same state of the heme iron. The similar data at both pH values thus served as a significant control for the reproducibility of the measurements on different samples. The data were fit to the Orbach relaxation mechanism over the range 2–3.7 K to give zero-field splitting ($2D/k$) of 29.6 (±0.2) K for wild-type CCP and 26.7 (±0.1) K for D235E. Also shown in Figure 9 are data for horseradish peroxidase, which gave a value of 32.5 (±0.1) K. This value is about 20% lower than that obtained previously for horseradish peroxidase by saturation recovery (Colvin et al., 1983) and may reflect some systematic difference between the two methods. Zero-field splittings were also obtained for the species giving rise to the axial ($g = 6.1$) EPR signal of these species. The axial high-spin forms of the wild-type enzyme and the Asp-235 mutants (Table II) have a smaller zero-field splitting parameter compared with that of the rhombic form, and only small differences are observed between the variants. Measurements at pH 5 on the axial signal at $g = 6.1$ gave $2D/k$ values of 23.2, 23.4, 21.6, and 22.3 K for wild-type CCP, D235E, D235N, and D235A, respectively.

DISCUSSION

This study was undertaken to examine the critical role that has been proposed for the Asp-His-Fe triad of peroxidases. Our observations support these proposals about the importance of this interaction in making a heme enzyme behave specifically like a peroxidase. By making the following three general statements, we may interpret our spectroscopic and functional data: (1) Wild-type CCP containing Asp-235 contributes a structurally and functionally important hydrogen bond to both His-175 and Trp-191 (Finzel et al., 1984). The interaction with His-175 is carefully optimized in strength and geometry to effectively deprotonate the N_δ position of His-175. The interaction with the Trp-191 free radical site serves to restrict its side-chain conformation in an orientation that is energetically unfavorable, but may provide an efficient mechanism for electron transfer into and out of the heme. (2) The mutations D235N and D235A completely disrupt the hydrogen-bonding interaction, leaving a normal, uncharged imidazole ligand axial to the iron. This dramatically alters the coordination state, redox potential, electronic structure, and function of the enzyme. Loss of the hydrogen bond to Trp-191 by either mutation results in its relaxation to a more energetically favorable orientation. This, however, significantly changes the critical coupling of the Trp-191 free radical center with the heme active site (Houseman et al., 1993). (3) The replacement of Asp-235 for Glu results in a very small displacement of the carboxylate and introduces only subtle changes in the geometry of its interactions with both Trp-191 and His-175. However, our results strongly suggest that the proton is no longer shared between Glu-235 and His-175, but instead remains essentially with the histidine. This results in many significant effects on the reduction potential, iron ligand field strength, and strength of coupling between the ferryl heme and the Trp-191 free radical.

State of the Hydrogen Bond in Wild-Type and Asp-235 Mutants. We have shown that the D235E mutation introduces only subtle changes at the active site, yet these small changes appear to have very significant consequences. The similar placement of the carboxylate in this mutant with respect to the wild-type enzyme is remarkable by consideration of the observed shift of the helix bearing residue 235. Our interpretation of the effects of the D235E mutation on the hydrogen-bonding geometry are presented in Figure 10. Little change is observed in the hydrogen bond distances between Glu-235 and either His-175 or Trp-191. However, the small twist in the carboxylate, and the corresponding rotation of His-175

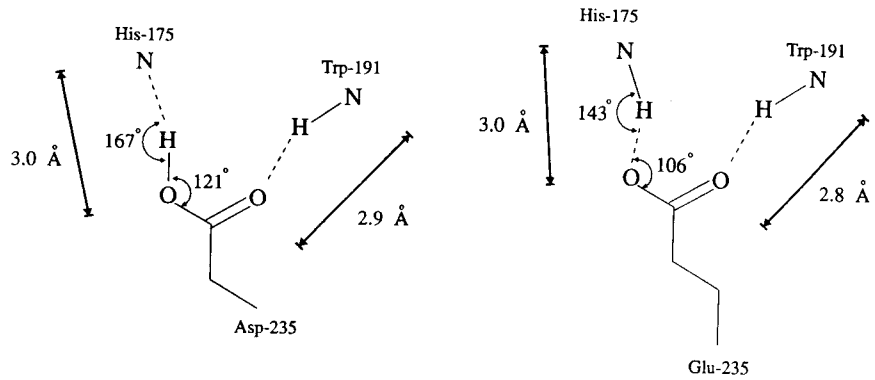

FIGURE 10: Schematic model depicting the structural effect of the D235E mutation on the His-175 hydrogen bond. The mutation does not significantly alter the hydrogen bond distance between Glu-235 and either His-175 or Trp-191. However, the subtle change in geometry may significantly affect the strength of this bond. A nearly ideal geometry is observed in the wild-type enzyme (Asp-235), in which the proton is well placed for interaction with the syn oxygen orbital containing a lone pair. As a result His-175 may essentially be deprotonated to the imidazolate. This geometry is altered in the D235E mutant and may cause the proton to reside predominantly on the histidine. The bond distances were measured from the refined crystal structures. In order to estimate the bond angles, a proton was placed on His-175 of the refined structures, and the angles to this inferred proton were measured.

(Figure 4) alters the geometry of the His-175 hydrogen bond. To illustrate this effect, protons were placed on the N_δ position of His-175 in the refined structures of CCP(MKT) and D235E, and the inferred H-bond geometries were measured from these protons. As shown in Figure 10, CCP(MKT) contains a nearly ideal H-bond geometry in which the N_ϵ–H–O angle is near 180°, and the C–O–H angle is essentially 120°. The proton is thus well positioned near the syn lone pair of the oxygen atom. These angles have been altered in the D235E mutant, with the C–O–H angle now at only 106°. Thus, although the distance between the carboxylate and His-175 is not significantly altered, the small observed change in the hydrogen bond geometry would be expected to significantly attenuate the strength of this interaction.

Our results indicate that the presence or strength of the Glu-His hydrogen bond of D235E can be modulated in solution. Resonance Raman data on the Fe^{2+} forms show that D235E exhibits an effect on the His–Fe mode in much the same way as D235N and D235A. The ferrous forms of D235N, D235A, and D235E each have resonance Raman spectra (G. Smulevich, personal communication) in which the Fe–histidine stretching bands at 233–246 cm^{-1} have shifted to approximately 205 cm^{-1} as reported previously for D235N (Smulevich et al., 1988). Although a native-like interaction with His-175 is not possible for D235N and D235A, it is significant that D235E retains a carboxylate in nearly the same position as in the wild-type enzyme. Thus, the small change in hydrogen bond geometry for D235E appears to be sufficient to alter the special character of the histidine–iron linkage, and this mutant, in the Fe^{2+} state, behaves as though the hydrogen bond has been disrupted. However, our EPR results of the Fe^{3+} state show evidence for a much more native-like environment. Although each of the mutants exhibits an axial $g = 6$ EPR signal, D235E is unique in that glycerol induces the rhombic signal observed for wild-type enzyme. As the similar effects of glyercol and MPD (used for crystallization) as agents stabilizing the 5-coordinate form of CCP have been noted (Smulevich et al., 1989), this state most closely mimics the conditions under which the crystal structures were determined. The axial and rhombically distorted EPR signals have been previously interpreted (Hori & Yonetani, 1985) as arising from the 6-coordinate and 5-coordinate high-spin states, respectively, yet they might more accurately describe the strength of the proximal histidine ligation. The strong imidazolate ligand resulting from the fully intact Asp-His interaction may introduce significant rhombic distortion to the predominantly axial g-tensor in much the same way that such anisotropy is controlled by the imidazole in low-spin hemes (Palmer, 1983; Quinn et al., 1987). Thus, the rhombic signals observed for wild-type CCP, D235E (glycerol), and other peroxidases (Maltempo et al., 1979) may indicate the presence of an intact hydrogen bond to His-175.

Changes in the state of the hydrogen bond to His-75 are also indicated in the pH-induced high- to low-spin transitions observed for these mutants. The D235N and D235A exist at low pH in a mixture of 6-coordinate high-spin and low-spin forms, and only D235E can be induced into a partially 5-coordinate configuration in the presence of glycerol. D235N and D235A go through two low-spin forms (ls1 and ls2), while D235E appears to resist formation of ls1 and converts directly to ls2. The sixth ligand of these mutants at pH 6 is the distal H_2O (see above) (Wang et al., 1990), and it has been proposed that the transition to the ls1 form is the result of the deprotonation of this H_2O to give the low-spin ferric hydroxyl complex (Smulevich et al., 1991). It thus appears that complete removal of the hydrogen bond (D235N and D235A) facilitates hydroxyl ligand formation, while the weakened hydrogen bond of D235E appears to retain sufficient strength to prevent this transition. Less is known about the conversion to the ls2 form, but it has been suggested (Smulevich et al., 1991) that this is associated with a distal conformational change which brings His-52 into position to displace the OH^- sixth ligand.

One of the important observations of this study is that despite the evidence for the weak hydrogen bond in D235E and the resulting effects that the substitution has on redox potential and electronic structure, this mutant retains significant catalytic competence. Thus, the critical role of this hydrogen bond for peroxidase function may not be as much in its demonstrated control of the redox potential as in its ability to maintain the reactive 5-coordinate high-spin heme configuration. The strong ligand provided by the partially deprotonated His-175 may help to restrict movement of the iron into the heme plane and thus prevent coordination by H_2O or His-52. This role of Asp-235 as a tether for His-175 was proposed along with the observation that the C_α and C_β atoms of His-175 are positioned so that the His-175 might move from side to side, but would be restricted in its movement toward the iron (Finzel et al., 1984). It is of considerable interest that replacement of the histidine ligand with glutamine (H175Q) results in an active high-spin enzyme (Sundaramoorthy et al., 1991). It is uncertain whether this mutant

contains a 5-coordinate heme or whether the coupling between the Trp-191 free radical and the heme is similar to wild-type enzyme, but it may be significant that H175Q was observed to form a hydrogen bond with Asp-235.

Coupling of the Trp-191 Free Radical to the Heme. Although the free radical species associated with the ES complex has been identified as Trp-191 (Sivaraja et al., 1989), important questions remain about its properties and how it communicates with the heme. For example, CCP contains two Trp residues in close contact with the heme (Trp-51 on the distal heme face and the proximal Trp-191), yet the free radical of wild-type CCP resides completely with Trp-191 (Sivaraja et al., 1989). A specific mechanism must therefore exist to efficiently promote Trp-191 oxidation, but it has not been established how this mechanism operates. A related question concerns the mechanism and strength of the coupling between the $S = {}^1/_2$ spin of the Trp radical and the $S = 1$ ferryl heme center. This coupling is generally considered to be the cause of the rapid spin relaxation, breadth, and unusual g values of the Trp-191 radical (Hoffman et al., 1981), although no satisfactory explanation of these properties existed until recently (Houseman et al., 1993).

This study demonstrates that the nature of the coupling between the Trp-191 site and the heme is very sensitive to the state of the Asp-His-Fe interaction. It has been shown that oxidation of the D235N mutant with H_2O_2 results in a narrow EPR signal which nevertheless showed a temperature-dependent relaxation (Fishel et al., 1991). While these results are consistent with our observations for D235N and D235A, it is not clear whether this narrow signal is a result of (1) the minority signal that is not associated with Trp-191 (Hori & Yonetani, 1985; Goodin et al., 1987), (2) a Trp-191 species with altered properties, or (3) a mixture of both. In addition, even if this signal were associated with Trp-191, it would not be possible to conclude that the altered signal was specifically the result of the loss of the hydrogen bond to Asp-235, because this mutation results in a complete reorientation of the Trp-191 ring. It is therefore significant that the D235E mutant shows a dramatically altered Trp-191 radical in spite of the nearly identical structure near this site. Essentially no difference in electron density is observed near Trp-191, and only a small change is seen in the geometry of the Glu-His interaction. As for the wild-type enzyme, the EPR signal of D235E ES shows the characteristics of an axial g-tensor. However, the sense of the g anisotropy is reversed with respect to the wild-type enzyme, so that $g_\parallel < g_\perp$ for D235E. Although changes in the line width for the apparent $g_\parallel = 2.04$ feature were noted for a number of mutations around the Trp-191 site (Fishel et al., 1991), none of these mutants showed this qualitative behavior.

The unusual properties of the ES EPR signal have recently been quantitatively described in terms of an exchange distribution model in which small fluctuations about the average structure produce a distribution of exchange couplings between the centers (Houseman et al., 1993). It was found that two such distributions were sufficient to account for the properties of the wild-type ES radical and that one of these distributions appeared to be absent in the D235E mutant. We therefore suggest that the two distributions observed for the wild-type enzyme correspond to the two states of hydrogen bonding between Asp-235 and His-175 in which the proton resides alternately on the Asp and the His. Such a double potential well for this proton has been proposed in the reduced state of CCP on the basis of the multiple Fe–His modes observed by resonance Raman spectra (Smulevich et al., 1988). For the D235E mutant, the hydrogen bond between Glu-235 and His-175 remains intact, but it is weakened to the point that the proton resides essentially with His-175. Thus, only one of the two coupling modes is observed between the Trp-191 radical and the heme.

Asp-His-Fe Control over Redox Potentials. The observed increase by approximately 100 mV upon removal of Asp-235 represents a significant fraction of the variability observed for the class of naturally occurring peroxidases (Millis et al., 1989). This illustrates one of the principal mechanisms by which evolutionary variation has been able to modulate the reduction potential without introducing changes in the highly conserved distal pocket. We wished to distinguish between alternative mechanisms by which Asp-235 could control the redox properties of this enzyme. The charge on the buried carboxylate near the heme center will alter the electrostatic free energy of the net +1 charge on the ferric porphyrin as determined by the Coulombic interaction and the local dielectric medium. Such effects have been characterized for mutants for myoglobin (Varadarajan et al., 1989a,b) and cyt b_5 (Rodgers & Sligar, 1991). A decrease of 200 mV in the midpoint reduction potential of myoglobin was observed by introducing a carboxylate into the distal heme environment (Varadarajan et al., 1989a). The importance of solvation to the electrostatic contribution of redox potentials has also been shown for iron–sulfur proteins (Langen et al., 1992). A more specific role would involve distribution of charge onto the partially deprotonated histidine, which would in turn direct delivery of charge to the iron through increased metal covalency. We now show that both of these mechanisms appear to operate in the case of CCP. For the mutaton D235E, the carboxylate remains in a position (Figure 4) that indicates that it is a hydrogen bond acceptor from both His-175 and Trp-191. An increase in the redox potential of approximately 100 mV is observed for the two mutants which removes both the hydrogen bond and the charge (D235N and D235A). About 70% of this increase is realized by retaining the carboxylate (D235E) but without the critical positioning necessary for a strong hydrogen bond. This is consistent with the suggestions that His-175 is deprotonated in the wild-type enzyme and that the proton resides effectively on His-175 in the D235E mutant and thus indicates a significant contribution of convalency in the control of electrochemical potential by this interaction. Quantitative calculations of the contribution of electrostatic and dielectric effects in these structures are needed to evaluate the relative contributions made by His-175 deprotonation and electrostatics, and such studies are planned for the future. Nevertheless, these data demonstrate that small structural variations from one type of peroxidase to another which modulate the strength of the axial histidine hydrogen bond could easily account for the considerable range of midpoint potentials found for this class of enzymes.

To evaluate the operation of this through-bond mechanism, we considered that alteration of the Asp-235 hydrogen bond might modify the strength or symmetry of the iron ligand field in a measurable way. Disruption of the hydrogen bond to His-175 should cause a decrease in the energy of the d_{z^2} orbital if the histidine–iron bond is significantly weakened. The resulting increase in energy of the lowest-lying excited quartet state ($^4A_2$) would reduce the extent of its mixing with the ground electronic state ($^6A_1$) and would thus lower the zero-field splitting ($2D$) of the $S = {}^5/_2$ ferric state of the enzyme (Schulz et al., 1984). There are two high-spin ferric signals to consider in these samples (Figure 2). As discussed above, the rhombically distorted axial signal with components

at $g = 6.59$ and 5.22 is observed for the wild-type enzyme and for the D235E mutant in the presence of glycerol and may correspond to those molecules with an intact hydrogen bond to His-175. The axial signal with $g = 5.95$ is observed for the D235A and D235N mutants and to a small extent in wild-type CCP and D235E. This signal has been shown to be characteristic of the 6-coordinate forms of CCP, such as the "aged" protein and the high-spin fluoride complex (Yonetani & Anni, 1987), and may in fact represent centers in which the Asp-235 hydrogen bond is broken. Thus, we would predict that the zero-field splitting should be larger for the rhombically distorted signals than for the axial species. In addition, we might expect to observe a more subtle difference in the rhombic signals of wild-type CCP and D235E.

The measured values of the zero-field splitting are fully in accord with these predictions. The data shown in Table II indicate that each of the states containing the axial EPR signal give roughly equal values of $2D/k$ which are 7–8 K lower than observed for the species represented by the rhombic signal. The mutation D235E results in a small but signiciant decrease in the zero-field splitting with respect to CCP(MKT) for the state giving the rhombic signal. This is expected for a weaker iron–histidine bond. We note that the zero-field splittings observed for these proteins appear to be correlated with the observed reduction potentials (Table II), indicating that the ligand field strength is contributing to the control over reduction potential. We also note that the very negative redox potential of HRP (–278 mV) and large zero-field splitting may result from an unusually strong proximal hydrogen bond in this enzyme.

The measurements of the iron zero-field splitting have proven to be an important factor in the interpretation of the effects of ligand field strength upon the redox properties of this enzyme. For example, it can be expected that a Cu^{2+} protein with a strained ligand geometry would have a higher reduction potential than similar small-molecule complexes. This is because the geometrical preferences of Cu^{2+} are more stringent than those of Cu^{+}, which obtains no ligand field stabilization from geometrical distortion. However, in the case of iron, both Fe^{2+} and Fe^{3+} prefer octahedral geometries, and thus the strength of the ligand donor is more important than geometry for defining its redox properties. Such a relationship has been observed for $P_{450_{cam}}$, where the substrate-induced spin-state transition was correlated with its reduction potential (Fisher & Sligar, 1985). In this case, the reduction potential decreased as the fraction of low-spin species was increased, as expected for an increase in ligand field strength. However, for CCP, we have observed that disruption of the Asp-235 hydrogen bond to His-175 results in a decrease in zero-field splitting and an increase in E_m, as expected for a weaker axial Fe–His bond, but these mutations also cause an increased propensity to form low-spin states. It appears that, for the case of CCP, disruption of the Asp-His interaction results in a weaker Fe–His bond, yet affords His-175 with the additional flexibility to follow the iron into the plane of the porphyrin, where hydroxyl coordination and heme core size effects result in the spin-state transition.

pH Dependence of the Reduction Potentials. The E_m vs pH curves for heme peroxidases show a decreasing potential with increasing pH that implies that reduction is accompanied by a protonation event. The site of this protonation has not been identified, but such a dependence has been conferred upon mylglobin by the introduction of an Asp or Glu into the distal heme environment (Varadarajan, 1989a). This suggests that the protonation observed upon CCP reduction may occur at Asp-235. The relatively pH-independent redox potentials below pH 6.5 for the Asp-235 mutants support this conclusion. However, resonance Raman data on reduced CCP indicate a strong Asp-His interaction and argue against a protonated Asp-235 (Smulevich et al., 1988). Many peroxidases exhibit two breaks in the E_m vs pH curve, which represent ionizations with differing pK values in the reduced and oxidized states (Ricard et al., 1972). An ionization of the reduced enzyme is observed in the redox curves with $pK_r = 7.4$, 6.3, 6.7, and 7.5 for HRP (Harbury, 1957), turnip PO1 (Ricard et al., 1972), lignin PO (Millis et al., 1989), and CCP (Conroy et al., 1978), respectively. This transition is associated with changes in optical spectra of the reduced enzyme that have recently been shown to reflect a two-proton conversion of the reduced enzyme from a 5-coordinate high-spin to a 6-coordinate low-spin form in CCP (Conroy et al., 1978; Miller et al., 1990). One study has suggested that this ionization of the ferrous enzyme represents a conformational change that results in the coordination of the distal His-52 to the heme iron (Smulevich et al., 1991).

The second break that is sometimes observed in the E_m vs pH profile occurs with $pK_o = 10.6$ and 10.2 for HRP (Harbury, 1957) and turnip PO1 (Ricard et al., 1972), respectively. This ionization was not observed for CCP or lignin PO within the pH range accessible to the electrochemical titrations. For HRP, this ionization corresponds to the alkaline transition of the oxidized enzyme to a low-spin species. Thus, each of these ionizations (pK_o and pK_r) appears to reflect a similar structural event, namely, the high- to low-spin transition for the oxidized and reduced states. Although our data for CCP(MKT) do not extend far enough to resolve the $pK_r = 7.5$ transition (which was only partially resolved in an earlier study of CCP (Conroy et al., 1978)), the optical spectra of the reduced states indicate an ionization at about pK = 7.6 for both CCP(MKT) and D235N. This is consistent with the results of Miller (Miller et al., 1990) and Smulevich (Smulevich et al., 1991). The most unusual feature in the E_m vs pH profiles of the Asp-235 mutants is the appearance of $pK_o \approx 6.5$, which matches the observed conversion of the oxidized state to the ls2 low-spin state (pK = 6.8). We thus propose that the pK_r and pK_o ionizations appearing on the E_m vs pH profiles of the peroxidases represent the high- to low-spin (ls2) transitions of the reduced and oxidized species and that for wild-type CCP, $pK_r = 7.5 < pK_o \approx 10$, but for the Asp-235 mutants pK_o 6.8 < $pK_r = 7.5$. If the sixth axial ligand in the ls2 state is hydroxyl, the pH dependence of the redox potential above the pK_o transition would represent the protonation of the hydroxyl as the 5-coordinate Fe^{2+} state is formed. If the ls2 state is characterized by bis-histidine coordination as previously suggested (Smulevich et al., 1991), the site of protonation remains to be assigned, and additional studies are indicated.

CONCLUSION

The importance of the Asp-His interaction as a structural element conferring unique physical or catalytic properties upon an enzyme active site has been clearly demonstrated for the serine proteases and has been proposed for many zinc enzymes. These studies show that the analogous interaction with the proximal histidine of CCP represents an important factor in regulating its coordination, electronic, and redox properties. The interaction serves two important roles: to modify the properties of the histidine as an axial heme ligand and to control the coupling of the Trp-191 free radical center with the heme. The very small structural alteration (D235E)

introduced at the active site of CCP is all that is necessary to (1) increase the reduction potential by approximately 70 mV, (2) alter the coupling of the Trp-191 free radical to the heme, (3) cause the facile pH-dependent conversion to the low-spin (ls2) species, and (4) alter the strength of the ligand field induced zero-field splitting of the heme. This result offers a significant view of the mechanism and subtlety with which the active site structure of the peroxidases exerts control over these properties.

ACKNOWLEDGMENT

We thank Prof. Giulietta Smulevich for kindly collecting resonance Raman spectra of the CCP mutants and Prof. Brian Hoffman, Dr. Gerard Jensen, Dr. John Tainer, Prof. James Roe, and Prof. Tom Poulos for numerous discussions.

REFERENCES

Abragam A., & Bleaney, B. (1986) in *Electron Paramagnetic Resonance of Transition Ions*, Dover, New York.
Brünger, A. T., Kuriyan, J., & Karplus, M. (1987) *Science 235*, 458.
Christianson, D. W., & Alexander, R. S. (1989) *J. Am. Chem. Soc. 111*, 6412.
Churg, A. K., & Warshel, A. (1986) *Biochemistry 25*, 1675.
Colvin, J. T., Rutter, R., Stapleton, H. J., & Hager, L. P. (1983) *Biophys. J. 41*, 105.
Conroy, C. W., Tyma, P., Daum, P. H., & Erman, J. E. (1978) *Biochim. Biophys. Acta 537*, 62.
Dawson, J. H. (1988) *Science 240*, 433.
Doeff, M. M., Sweigart, D. A., & O'brien, P. (1983) *Inorg. Chem. 22*, 851.
Finzel, B. C., Poulos, T. L., & Kraut, J. (1984) *J. Biol. Chem. 259*, 13027.
Fishel, L. A., Farnum, M. F., Mauro, J. M., Miller, M. A., Kraut, J., Liu, Y. J., Tan, X. L., & Scholes, C. P. (1991) *Biochemistry 30*, 1986.
Fisher, M. T., & Sligar, S. G. (1985) *J. Am. Chem. Soc. 107*, 5018.
Fisher, M. T., & Sligar, S. G. (1987) *Biochemistry 26*, 4797.
Goodin, D. B., Mauk, A., G., & Smith, M. (1987) *J. Biol. Chem. 262*, 7719.
Goodin, D. B., Davidson, M. G., Roe, J. A., Mauk, A. G. & Smith, M. (1991) *Biochemistry 30*, 4953.
Groves, J. T., & Nemo, T. E. (1983) *J. Am. Chem. Soc. 105*, 5786.
Harbury, H. A. (1957) *J. Biol. Chem. 225*, 1009.
Hoffman, B. M., Roberts, J. E., Kang, C. H., & Margoliash, E. (1981) *J. Biol. Chem. 256*, 6556.
Hori, H., & Yonetani, T. (1985) *J. Biol. Chem. 260*, 349.
Houseman, A. L. P., Doan, P. E., Goodin, D. B., & Hoffman, B. M. (1993) *Biochemistry* (in press).
Howard, A. J., Gilliland, G. L., Finzel, B. C., Poulos, T. L., Ohlendorf, D. H., & Salemme, F. R. (1987) *J. Appl. Crystallog. 20*, 383.
Ikeda-Saito, M., & Prince, R. C. (1985) *J. Biol. Chem. 260*, 8301.
Kraulis, P. J. (1991) *J. Appl. Crystalogr. 24*, 946.
Langen, R., Jensen, G. M., Jakob, U., Stephens, P. J. & Warshel, A. (1992) *J. Biol. Chem.* (in press).
Lee, W. A., Calderwood, T. S., & Bruice, T. C. (1985) *Proc. Natl. Acad. Sci. U.S.A. 82*, 4301.
Makino, R., Chiang, R., & Hager, L. P. (1976) *Biochemistry 15*, 4748.
Maltempo, M. M., Ohlsson, P.-I., Paul, K.-G., Petersson, L., & Ehrenberg, A. (1979) *Biochemistry 18*, 2935.
McRee, D. E. (1992) *J. Mol. Graphics 10*, 44.
Miller, M. A., Coletta, M., Mauro, J. M., Putnam, L. D., Farnum, M. F., Kraut, J., & Taylor, T. G. (1990) *Biochemistry 29*, 1777.
Millis, C. D., & Tien, M. (1989) *Biochemistry 28*, 8484.
Nicola, N. A., Minasian, E., Appleby, C. A., & Leach, S. J. (1975) *Biochemistry 14*, 5141.
Palmer, G. (1983) in *Iron Porphyrins*; *Part II* (Lever, A. B. P., & Gray, H. B., Eds.) p 43, Addison-Wesley, Reading, MA.
Pease, E. A., Andrawis, A., & Tien, M. (1989) *J. Biol. Chem. 264*, 13531.
Pribnow, D., Mayfield, M. B., Nipper, V. J., Brown, J. A. & Gold, M. H. (1989) *J. Biol. Chem. 264*, 5036.
Quinn, R., Valentine, J. S., Byrn, M., P., & Strouse, C. E. (1987) *J. Am. Chem. Soc. 109*, 3301.
Rees, D. C. (1980) *J. Mol. Biol. 141*, 323.
Ricard, J., Mazza, G., & Williams, R. J. P. (1972) *Eur. J. Biochem. 28*, 566.
Rodgers, K. K., & Sligar, S. G. (1991) *J. Am. Chem. Soc., 113*, 9419.
Satterlee, J. D., Erman, J. E., Mauro, J. M., & Kraut, J. (1990) *Biochemistry 29*, 8797.
Saunders, B. C. (1973) in *Inorganic Biochemistry* (Eichhorn, G. L., Ed) Vol. 2, p 988, Elsevier, Amsterdam.
Scholes, C. P., Isaacson, R. A., & Feher, G. (1971) *Biochim. Biophys. Acta 244*, 206.
Schulz, C. E., Rutter, R., Sage, J. T., Debrunner, P. G., & Hager, L. P. (1984) *Biochemistry 23*, 4743.
Sivaraja, M., Goodin, D. B., Smith, M., & Hoffman, B. M. (1989) *Science 245* (4919), 738.
Smulevich, G., Mauro, J., Fishel, L. A., English, A. M., Kraut, J., & Spiro, T. G. (1988) *Biochemistry 27*, 5477.
Smulevich, G., Mantini, A., English, A. M., & Mauro, J. (1989) *Biochemistry 28*, 5058.
Smulevich, G., Miller, M. A., Kraut, J., & Spiro T. G. (1991) *Biochemistry 30*, 9546.
Spiro, T. G., Smulevich, G., & Su, C. (1990) *Biochemistry 29*, 4497.
Stankovich, M. T. (1980) *Anal. Biochem. 109*, 295.
Stein, P., Mitchell, M., & Spiro, T. G. (1980) *J. Am. Chem. Soc. 102*, 7795.
Stephens, P. J. (1976) *Adv. Chem. Phys. 35*, 197.
Sundaramoorthy, M., Choudhury, K., Edwards, S. L., & Poulos, T. L. (1991) *J. Am. Chem. Soc. 113*, 7755.
Swartz, J. C., Stanford, M. A., Moy, J. N., Hoffman, B. M., & Valentine, J. S. (1979) *J. Am. Chem. Soc. 101*, 3396.
Tainer, J. A., Roberts, V. A., & Getzoff, E. D. (1992) *Curr. Opin. Biotechnol. 3*, 378.
Tien, M. & Kirk, T. K. (1983) *Science 221*, 661.
Traylor, T. G., Lee, W. A., & Stynes, D. V. (1984) *J. Am. Chem. Soc. 106*, 755.
Valentine, J. S., Sheridan, R. P., Allen, L. C., & Kahn, P. C. (1979) *Proc. Natl. Acad. Sci. U.S.A. 76*, 1009.
Varadarajan, R., Zewert, T. E., Gray, H. B., & Boxer, S. G. (1989a) *Science 243*, 69.
Varadarajan, R., Lambright, S. G., & Boxer, S. G. (1989a) *Biochemistry 28*, 3771.
Wang, J. M., Mauro, J. M., Edwards, S. L., Oatley, S. J., Fishel, L. A., Ashford, V. A., Xuong, N. H., & Kraut, J. (1990) *Biochemistry 29*, 7160.
Warshel, A., Naray-Szabo, G., Sussman, F., & Hawang, J.-K. (1989) *Biochemistry 28*, 3629.
Yonetani, T. (1976) in *The Enzymes* (Boyer, P. D., Ed.) Vol. 13, p 345, Academic, New York.
Yonetani, T. & Anni, H. (1987) *J. Biol. Chem. 262*, 9547.